HEPATOLOGY
Official Journal of the American Association for the Study of Liver Diseases

Radiologic Course of Primary Sclerosing Cholangitis: Assessment by Three-Dimensional Magnetic Resonance Cholangiography and Predictive Features of Progression

Ana Ruiz,[1] Sara Lemoinne,[2] Fabrice Carrat,[3] Christophe Corpechot,[2] Olivier Chazouillères,[2] and Lionel Arrivé[1]

Magnetic resonance imaging (MRI) with magnetic resonance cholangiography (MRC) has become the radiologic standard of reference for diagnosis of primary sclerosing cholangitis (PSC). However, natural history of radiologic features of PSC is poorly known. In the current study, we aimed at analyzing the course of PSC using three-dimensional (3D) MRC and liver MRI to find predictive radiologic features of progression. PSC patients, followed up in our center, with at least two 3D MRCs performed in at least a 1-year interval, were retrospectively reviewed. We built an interpretation standard model to score precisely bile ducts and liver parenchyma features. The primary endpoint was overall radiologic course, including worsening, improvement, or stabilization. Radiologic features were analyzed by logistic regression. We reviewed 289 MRIs from 64 patients upon a mean radiologic follow-up of 4 years (range, 1-9). Radiologic features worsened in 37 patients (58%) and stabilized in 27 (42%); no patient showed improvement. Multivariate analysis resulted in two MRI progression risk scores, based on the combination of predictive radiologic features (score without gadolinium administration = 1 × dilatation of intrahepatic bile ducts + 2 × dysmorphy + 1 × portal hypertension; score with gadolinium administration = 1 × dysmorphy + 1 × parenchymal enhancement heterogeneity). These scores were associated with radiologic progression, with an area under the curve of 80 and 83% ± 4%. *Conclusion*: A majority of PSC patients develop radiologic aggravation upon MRI over 4 years. Two simple scores can predict radiologic progression.(HEPATOLOGY 2014;59:242-250)

Primary sclerosing cholangitis (PSC) is a rare chronic cholestatic liver disease with an overall incidence rate of 0.77 per 100,000 person-years.[1] This disease of unknown cause is commonly associated with inflammatory bowel disease (IBD) and characterized by progressive obliterative fibrosis of the biliary tree.[2] Although the natural course may vary from one patient to another, PSC is often progressive, leading to biliary cirrhosis and its complications. A diagnosis of PSC is performed in patients with biochemical cholestasis not otherwise explained, when cholangiography shows multifocal strictures and segmental dilatations and when causes of secondary sclerosing cholangitis (especially immunoglobulin G–associated cholangitis) have been excluded.[3,4]

Endoscopic retrograde cholangiography (ERC) has been the standard of reference in diagnosing PSC, but is associated with complications, such as pancreatitis

Abbreviations: 2D, two-dimensional; 3D, three-dimensional; AUC, area under the curve; CBD, common bile duct; CCA, cholangiocarcinoma; ERC, endoscopic retrograde cholangiography; HIV, human immunodeficiency virus; IBD, inflammatory bowel disease; IHBD, intrahepatic bile ducts; LHD, left hepatic duct; MIP, maximum intensity projection; MRC, magnetic resonance cholangiography; MRI, magnetic resonance imaging; MRS, Mayo Risk Score; NPV, negative predictive value; PH, portal hypertension; PPV, positive predictive value; PSC, primary sclerosing cholangitis; RHD, right hepatic duct; ROC, receiver operating characteristic; UDCA, ursodeoxycholic acid.

From the [1]APHP, Service de radiologie, Hôpital Saint Antoine, Paris, France and Université Pierre et Marie Curie (UPMC, Paris VI), Paris, France; [2]APHP, Service d'hépatologie, Hôpital Saint Antoine, Paris, France and Université Pierre et Marie Curie (UPMC, Paris VI), Paris, France; and [3]Inserm UMR-S 707, and Département de Santé Publique, Hôpital Saint-Antoine, Paris, France and Université Pierre et Marie Curie (UPMC, Paris VI), Paris, France.

Received April 9, 2013; accepted July 1, 2013.

and sepsis.[5] Description of cholangiographic features was based on several classifications, including those of Majoie et al.[6] and Craig et al.[7] Recently, because of its noninvasive nature and a similar diagnostic accuracy,[8-11] magnetic resonance cholangiography (MRC) has become the recommended radiologic modality for the diagnosis of PSC.[3] However, image analysis on MRC is still based on ERC classifications, despite major differences. Indeed, MRC allows evaluation of the ducts in their physiologic "resting" state (no bile duct tension) and visualization of the ducts proximal to a severe stricture. In addition and unlike ERC, magnetic resonance imaging (MRI) permits imaging of the liver and may identify alterations in hepatic morphology. MRI features of PSC have mainly been described using two-dimensional (2D) MRC,[12-14] but over the last decade, use of three-dimensional (3D) MRC has improved image quality and bile duct visualization.[15] Thus far, to date, no radiologic abnormalities classification has been published using 3D MRC.

Several prognostic models have been developed and the most popular is the Mayo Risk Score (MRS), which includes clinical and biological parameters.[16,17] However, because there is no consensus regarding the optimal model, their use is not recommended for predicting clinical outcomes in an individual patient.[5] A role for cholangiographic information in developing a prognostic model has been suggested. Using ERC, some researchers reported that high-grade intrahepatic strictures were associated with poor prognosis[7,18] and others found that dominant bile duct stenoses were associated with poor outcome.[19,20] Interestingly, Dutch investigators reported that cholangiographic scoring (derived from Majoie et al.'s classification) was inversely correlated with survival.[21] Nevertheless, the reproducibility of strictures grading in ERC may be questionable considering the contrast injection technique variability, thus making these classifications unsuitable for MRI. Using 2D MRC, no correlation was found between radiologic features and the MRS.[22] To date, no attempt has been made to identify the features predictive of disease progression on 3D MRC. Moreover, at present, there is no consensus on radiologic follow-up modalities in PSC, American and European recommendations simply stating that an abdominal ultrasound should be performed annually to detect mass lesions in the gallbladder.[3,4]

The policy of our center is to perform a routine 3D MRC once a year in PSC patients. Therefore, the aim of our study was to describe the radiologic course of PSC by using an MRI scoring system and to identify features able to predict the radiologic course of PSC.

Patients and Methods

Study Population. Our hospital institutional review board approved the review of radiologic and clinical data for this study. Informed consent was not required for this retrospective analysis.

Radiologic files from a series of patients with PSC from our center were retrospectively reviewed. These included MRI performed between December 2002 (implementation of 3D MRC in our center) and June 2011 (date of study termination) on patients followed up in the referral center for biliary inflammatory diseases of our hospital. Diagnosis of PSC in these patients was based on the aforementioned criteria.[3,4] MRIs from patients who had undergone at least two 3D MRCs with at least a 1-year interval between, for diagnostic purposes and/or as part of the follow-up (routine follow-up or work-up for clinical or biological changes), were included in the study. Exclusion criteria were small-duct PSC, autoimmune hepatitis PSC overlap syndrome, previous liver transplantation or significant hepatic comorbidities, such as associated hepatitis B or C, human immunodeficiency virus (HIV) infection, or nonalcoholic steatohepatitis (Fig. 1, flow chart).

MRI Technique. MRI was performed according to the protocol for 3D MRC previously described by our group.[23] Fasting for at least 4 hours before examination was required. Pineapple juice (400 mL 15 minutes before the examination) was used as a negative oral contrast agent. When performed, a 3D fat-suppressed T1-weighted ultrafast gradient-echo acquisition was done before and after intravenous administration of 20 mL of Gd-DOTA (Dotarem; Guerbet, Aulnay-sous-Bois, France), with hepatic arterial, portal

Address reprint requests to: Lionel Arrivé, M.D., Service de radiologie, Hôpital Saint Antoine, 184 rue du Faubourg Saint Antoine, 75012 Paris, France. E-mail: lionel.arrive@sat.aphp.fr; fax +33149282259.

View this article online at wileyonlinelibrary.com.

DOI 10.1002/hep.26620

Potential conflict of interest: Nothing to report.

Additional Supporting Information may be found in the online version of this article.

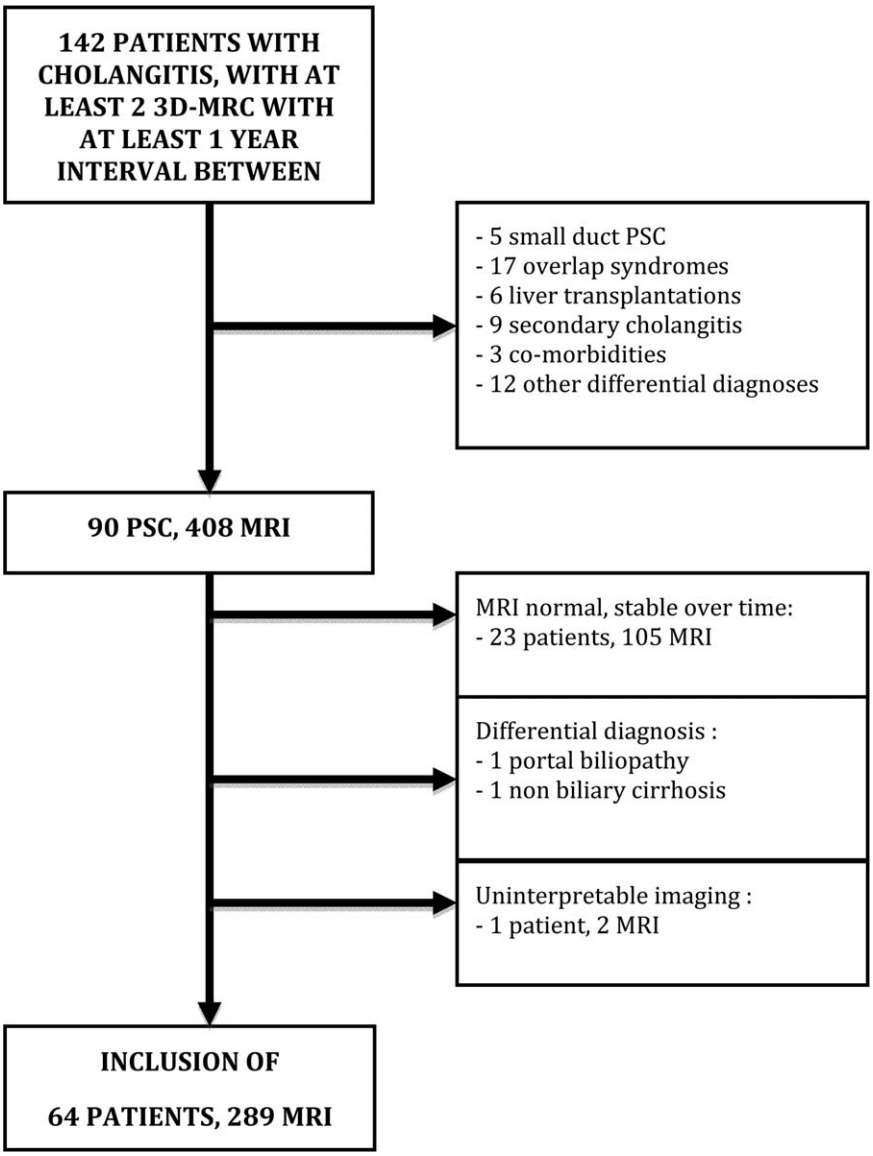

Fig. 1. Flow chart of the retrospective study done between January 2002 and June 2011.

venous, and equilibrium phase acquisition (respectively, 30 seconds, 80 seconds, and 3 minutes).

Image Analysis. Two abdominal radiologists (L.A. and A.R. with 25 and 5 years of experience in abdominal imaging) reviewed all MRIs in consensus. They were blinded to clinical information, such as associated IBD, diagnosis date of PSC, histological or ERC data, current treatment, and biochemical parameters.

Native images and 3D maximum intensity projection (MIP) reconstructions were analyzed on a Workstation, using the Carestream Picture Archiving and Communication System (version 11.32; Carestream Health, Rochester, NY). MIPs were analyzed on thick slabs of 10 or 20 mm, orientated in the acquisition plane. Based on Craig et al.'s classification[7] and on the degree of peribiliary enhancement described by Petrovic et al.,[22] an interpretation standard model was constructed. This model was then tested on 20 patients from a list of patients with PSC 3 months before the start of analysis to avoid recall bias (only 8 patients from this subset of 20 patients were after part of the study). In the model, the biliary tree was split into four portions: common bile duct (CBD); right hepatic duct (RHD); left hepatic duct (LHD); and intrahepatic bile ducts (IHBDs). The LHD, RHD, and CBD were considered as extrahepatic portions. The presence of strictures (present or absent) and grade (mild, $\leq$75%; severe, $>$75%) was defined for each portion. The length of the strictures was given for CBD, RHD, and LHD portions (band, 1-2 mm; segmental, 3-10 mm; confluent, $>$10 mm) and extent of liver involvement was given for IHBDs (localized,

≤25%; diffuse, >25%). Stricture was defined as a decrease in the diameter of a bile duct, and the stricture grade was evaluated as the minimum diameter at the level of stricture divided by the diameter of the duct below. Then, for each portion, we analyzed the presence of bile duct dilatation (normal values: IHBD, ≤3 mm; RHD and LHD, ≤6 mm; CBD, ≤10 mm), its degree (mild: IHBD = 4 mm; RHD and LHD = 7-8 mm; CBD = 11-14 mm; marked: IHBD, ≥5 mm; RHD and LHD, ≥9 mm; CBD, ≥15 mm), the presence of intraductal stones (present or absent), peribiliary enhancement at equilibrium phase (present or absent), and peribiliary enhancement thickness (<2 mm; 2-6 mm; >6-mm margin of enhancement surrounding the bile ducts).

Associated liver-related signs were recorded for all MRIs, including dysmorphy, such as significant atrophy of either the right or left hepatic lobe and/or marked lobulations of liver surface and/or increase of the caudate/right lobe ratio,[24] heterogeneity of enhancement on arterial phase, portal hypertension (PH; presence of portosystemic shunts with or without splenomegaly), gallbladder appearance (removed; normal size with length/width ≥2; dilated with biconvex contours or length/width <2), and lymph nodes (present if supracentimetric size or enlarged number). In addition, the presence of any lesion with suspicious signs of cholangiocarcinoma (CCA)[25] was investigated in each patient. The detection of a mass suspicious for carcinoma, of an abscess or of intraductal stones, was considered as a complication. Some examples of this semiology are illustrated in Supporting Figs. 1 and 2.

Primary Endpoint. MRIs from each patient taken during the follow-up period were analysed in chronological order. For each radiologic feature (stricture, dilatation, dysmorphy, and so on) from the interpretation standard model, points were given according to Supporting Table 1 and an addition of radiologic features was performed. For each patient, the primary endpoint was based on the comparison of the addition of radiologic features between first and last MRI, including worsening if the last addition was higher than the first, stability if addition was unchanged, and improvement if the last addition was lower than the first.

Statistical Analysis. Groups of patients were defined according to the primary endpoint. The chi-square test and the *t* test were used to confirm the comparability of the groups in terms of demographic data (sex and age), time between diagnosis of PSC and the first MRI (0, 1-2, or >2 years), and mean follow-up period.

We identified radiologic items associated with changes between any two successive MRIs (n and n+1) using logistic regression models adapted for dealing with within-subject correlated data.[26] The response/dependent variable was changes at MRI n+1 compared with MRI n. The radiologic item was value observed during MRI n. Time interval between the two MRIs was entered as an adjustment covariate and an exchangeable log odds ratio was introduced to take into account within-subject correlation. Each radiologic item was tested in a univariate model, and significant items were entered in a multivariate logistic model and selected using a backward procedure, retaining items with a P value <0.05.

To build the scores, regression coefficients of significantly associated items were rounded to their nearest integer and combined in a linear predictor, as previously recommended.[27] To estimate the predictive performance of a score, we estimated a logistic model as described above with the score as a predictor and we calculated the area under the receiver operating characteristic (ROC) curve (area under the curve; AUC) of the estimated model. We used a bootstrap technique with 100 resamples to correct from the optimism bias, as described by Steyerberg et al.[28] All analyses were performed with SAS statistical software (v9.3; SAS Institute Inc., Cary, NC).

Results

Study Population

MRIs of 142 patients with a diagnosis of sclerosing cholangitis and two or more 3D MRCs with at least a 1-year interval were reviewed. A number of patients did not enter the study mainly because of a diagnosis of small duct PSC or overlap syndrome (Fig. 1, flow chart). Finally, 64 patients were included in the study (289 MRI; 26 women and 38 men; mean age: 41.2 years). Liver biopsy was available in 59 patients (92%); extensive fibrosis or cirrhosis was present in 25%. A total of 45 patients (70%) had concurrent IBD (Crohn's disease: n = 23; ulcerative colitis: n = 19; unclassified colitis: n = 3). The median number of MRC per patient was 4 (range, 2-10) over a mean follow-up period of 3.9 years (range, 1-9). The first MRI was performed for diagnostic purposes in 21 patients (33%). For the others, the first MRI was part of the follow-up, performed 1-2 years after diagnosis in 14 patients (22%) and 3 years or more after diagnosis in 29 (45%). Mean time between diagnosis and inclusion was 2.5 years (range, 0-22). At the time of the first MRI, 47 patients (73%) were treated with ursodeoxycholic acid (UDCA) and during follow-up all patients were

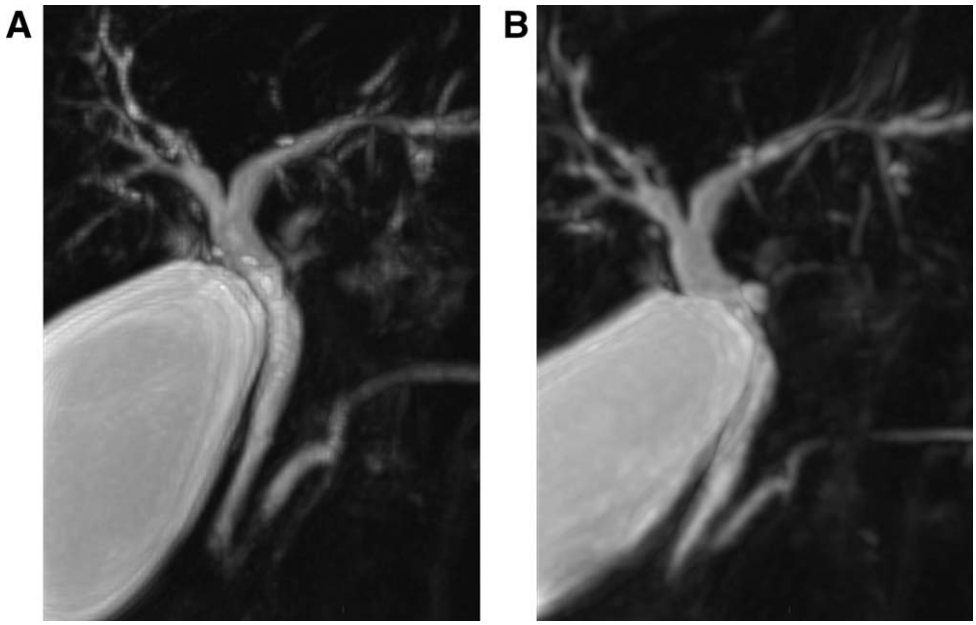

Fig. 2. Radiologic natural disease course. Stable disease: 42-year-old patient in 2004 (A) and 2009 (B). 3D MRCP MIP images showing diffuse intrahepatic bile ducts strictures without dilatation. No strictures or dilatation on common bile duct, right or left hepatic ducts. Dilated gallbladder, absence of intraductal stones. No peribiliary enhancement, no heterogeneity in parenchymal enhancement, no dysmorphy, no portal hypertension (not shown).

given UDCA, with a median dose of 15 mg/kg/day at entry.

MRI Descriptive Data

MRI With Contrast-Enhanced T1-Weighted Sequences. Almost every patient (94%; n = 60) had at least one MRI with contrast-enhanced T1-weighted sequence during follow-up. In total, 73.4% (212 of 289) of the 3D MRC group were followed by gadolinium administration.

Topography of Disease-Affected Areas. Fifty-four patients (84%) had both intra- and extrahepatic disease, 10 (16%) had intrahepatic disease only, and none had isolated extrahepatic disease.

Characteristic Features of the Disease on the First MRI. Regarding IHBD, 100% of patients had strictures, diffusely affecting the liver in 93.8%, with dilatation in 73.4% of cases (marked dilatation in 10.9% of cases). Regarding CBD, 70.3% of patients had strictures, confluent in 75.6% of cases, with dilatation in 4.7% of cases. Overall, 62.5% had at least one severe stricture (>75%) on extrahepatic bile ducts. Regarding liver parenchyma, 53.1% of patients showed dysmorphy, 51.4% parenchymal heterogeneity, and 19.4% PH (characteristic features shown in Supporting Table 2).

Characteristic Features of the Disease on the Last MRI. Regarding IHBD, strictures were diffusely distributed in the liver in 95.3% of patients, with dilatation in 78.1% of cases (marked dilatation in 34.4% of cases). Regarding CBD, 73.4% of patients had strictures, confluent in 83% of cases, with dilatation in 10.9% of cases. Overall, 70% had at least one severe stricture (>75%) on extrahepatic bile ducts. Regarding liver parenchyma, 57.8% of patients showed dysmorphy, 67.3% parenchymal heterogeneity, and 35.9% PH (characteristic features shown in Supporting Table 3).

Primary Endpoint on Overall Radiologic Course. The disease was stable in 27 patients (42%), worsened in 37 (58%), and improved in none of the patients (0%). The two patterns of radiologic disease course are illustrated in Figures 2 and 3. On the first MRI, the mean addition of radiologic features and standard deviation was 16.1 ± 5.0 points for worsening disease and 10.8 ± 5.7 points for stable disease. There was a significant difference between the two groups with a probability of $P < 0.001$. The mean addition of radiologic features for the last MRI in worsening disease was 20.2 ± 4.6 points, compared with 16.1 ± 5.0 points on the first MRI (see Supporting Figure 3, spaghetti plot). During follow-up, we never observed a discrepancy in evolution of radiologic features (i.e., worsening of one and improvement of another).

Comparability of the Two Groups. No significant difference was found between the two groups in terms of demographic data, time between diagnosis and first MRI available, and follow-up duration (see Supporting Table 4).

Group of Patients Showing Stable Disease on MRI (n = 27). First MRI features are presented in Supporting Table 5. Fifty-six percent of patients had CBD strictures, 60% dilatation of IHBDs, 6% peribiliary enhancement, 15% dysmorphy, 12% parenchymal enhancement heterogeneity after gadolinium administration, and 4% PH.

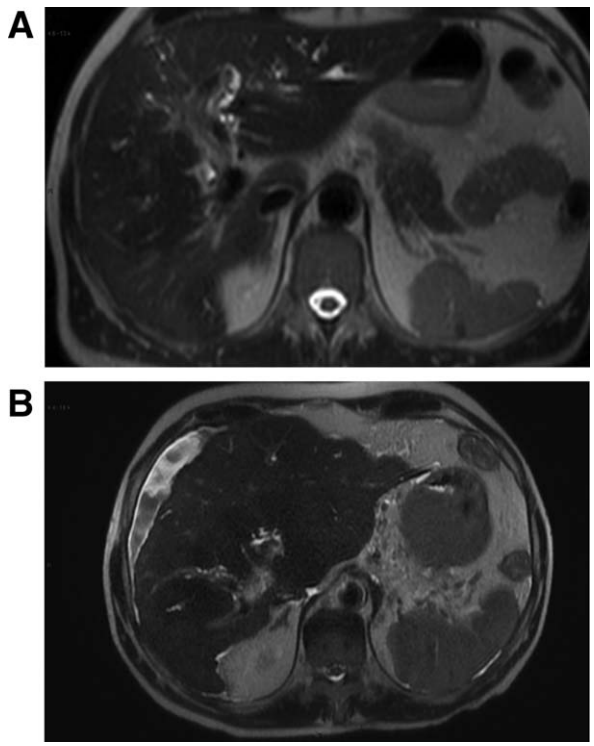

Fig. 3. Radiologic natural disease course. Worsening disease: 41-year-old patient in 2005 (A) and 2010 (B). T2-weighted images showing worsening on dysmorphy, with increase in caudate-right lobe ratio, lobulation of the liver contours, atrophy of posterior right lobe, hypertrophy of medial left lobe. Signs of portal hypertension with portosystemic shunts, intraperitoneal fluid, and increase in spleen size on B.

Group of Patients Showing Worsening Disease on MRI (n = 37). On average, lesions worsened at 1.5 years (range, 1-5); 26 patients (70%) showed first evidence of worsening on the MRI performed at 1 year, 9 (25%) on the MRI at 2-3 years, and 2 (5%) on the MRI at 4-5 years. First MRI features in this group are presented in Supporting Table 6. Eighty-one percent of patients had a CBD stricture, 87% dilatation of the IHBDs, 52% peribiliary enhancement, 81% dysmorphy, 85% parenchymal enhancement heterogeneity after gadolinium administration, and 31% PH.

Table 1. Comparison of First and Last MRI in Radiologically Worsening Patients

	First MRI	Last MRI	*P* Value
Stricture (n)	37	37	
CBD stricture	30	32	NS
CBD stricture >75%	17	26	<0.050
RHD stricture	31	33	NS
LHD stricture	26	30	NS
IHBD stricture	37	36	NS
IHBD stricture >75%	33	36	NS
Dilatation (n)	37	37	
CBD dilatation	1	5	NS
IHBD dilatation	32	35	NS
IHBD marked dilatation	5	20	<0.001
Gadolinium administration (n)	21	34	
CBD enhancement	6	16	NS
IHBD enhancement	11	21	NS
Intraductal stones (/n)	13/33	21/36	NS
Dysmorphy (/n)	30/37	33/37	NS
Liver enhancement heterogeneity (/n)	17/20	32/34	NS
PH (/n)	11/35	22/37	<0.020
Gallbladder dilatation (/n)	17/36	20/33	NS

Abbreviations: NS, not significant.

Table 2. Features Associated With Radiological Progression (Univariate Analysis)

	Regression Coefficient	95% Confidence Interval		*P* Value
Stricture				
CBD	0.16	−0.35	0.67	NS
RHD	0.42	−0.09	0.92	NS
LHD	0.07	−0.52	0.65	NS
IHBDs	1.11	0.15	2.08	<0.0500
Stricture length				
CBD	0.24	−0.10	0.57	NS
RHD	0.33	−0.05	0.71	NS
LHD	0.04	−0.32	0.41	NS
IHBD stricture spreading	24.31	–	–	N/A
Dilatation				
CBD dilatation	−0.75	−2.21	0.72	NS
RHD dilatation	0.65	−0.22	1.53	NS
LHD dilatation	0.58	−0.08	1.24	NS
IHBD dilatation	0.84	0.36	1.32	<0.0010
Gadolinium administration				
CBD enhancement	0.95	0.10	1.80	<0.0500
RHD enhancement	0.94	0.21	1.67	<0,0200
LHD enhancement	0.67	−0.11	1.45	NS
IHBD enhancement	0.88	0.05	1.72	<0.0500
Intraductal stones	0.44	−0.28	1.16	NS
Dysmorphy	2.15	1.21	3.10	<0.0001
Liver enhancement heterogeneity	2.71	1.65	3.77	<0.0001
PH	1.34	0.57	2.11	<0.0010
Gallbladder	0.12	−0.61	0.86	NS
Lymph nodes	0.83	0.22	1.45	<0.0100

NS, not significant; N/A, not available.

Comparison of First and Last MR Images From Evolutive Patients. Table 1 presents the radiologic features that differ between the initial and the final MRI in this group of patients. Significant differences can be observed concerning CBD high-grade strictures, marked dilatation of the IHBDs, and PH.

Tumoral Lesions. Five patients developed carcinomatous lesions: CCA of the CBD (n = 1); gallbladder CCA (n = 2); intrahepatic CCA (n = 1); and hepatocellular carcinoma (n = 1).

Predictive Factors of Radiologic Progression on MRI. By univariate analysis, seven parameters were significantly linked to radiologic worsening: IHBD strictures; IHBD dilatation; peribiliary enhancement; dysmorphy; parenchymal enhancement heterogeneity;

Table 3. Features Associated With Radiological Progression (Multivariate Analysis)

	Regression Coefficient	95% Confidence Interval		*P* Value
Without gadolinium				
IH dilatation	0.71	0.16	1.26	0.010
Dysmorphy	1.67	0.66	2.69	0.001
PH	0.84	0	1.70	0.050
With gadolinium				
Dysmorphy	2.12	0.89	3.34	0.001
Parenchymal heterogeneity	1.51	0.28	2.72	0.020

PH; and lymph nodes (Table 2). Interestingly, severe stricture (>75%) of extrahepatic bile ducts was not associated with worsening.

By multivariate analysis, there were three independent predictors of radiologic worsening (IHBD dilatation, PH, and dysmorphy) when MRI was performed without gadolinium administration and two (dysmorphy and parenchymal heterogeneity) when MRI was performed with gadolinium administration (Table 3).

MRI Progression Risk Score. To build progression risk scores (with or without gadolinium), the regression coefficient of the independent predictors was rounded to their nearest integer and combined in a linear predictor. The score was built to predict disease evolution in any two successive MRIs. We used 224 paired measurements of successive MRIs, of which 107 reported worsening whereas 117 reported stability. The results were as shown by the following equations:

$$\text{MRI progression risk score (without gadolinium)} = 1\times\text{dilatation IHBD} + 2\times\text{dysmorphy} + 1\times\text{PH}$$

$$\text{MRI progression risk score (with gadolinium)} = 1\times\text{dysmorphy} + 1\times\text{parenchymal enhancement heterogeneity}$$

For these calculations, IHBD dilatation was scored as 0 (≤3 mm), 1 (4 mm), or 2 (≥5 mm); dysmorphy, PH, and parenchymal heterogeneity were scored as 0 (absence) or 1 (presence). The without-gadolinium score can thus vary between 0 and 5 and the with-gadolinium score between 0 and 2.

The without-gadolinium score had a mean of 3.49 in the group with progression, compared to 1.74 in the stable disease group. The performance of the without-gadolinium score for predicting radiologic progression was assessed by ROC analysis showing an AUC of 80.2% ± 4%. With a threshold at 3 (score ≥3 or <3), this score had a sensitivity of 87%, a specificity of 63%, a positive predictive value (PPV) of 68%, and a negative predictive value (NPV) of 84% for predicting progression.

The with-gadolinium score had a mean of 1.86 in the group with progression, compared to 0.75 in the stable disease group. The performance of the with-gadolinium score in predicting radiologic progression was validated by ROC analysis showing an AUC of 83% ± 4%. With a threshold at 2 (score = 2 or <2), this score had a sensitivity of 91%, a specificity of 72%, a PPV of 74%, and an NPV of 90% for predicting progression.

Discussion

Use of an interpretation standard model with 3D MRC has allowed us to perform a systematic analysis of bile ducts and liver parenchyma in PSC patients over time. To the best of our knowledge, it is the first time such a model has been provided. Our population of highly selected patients with PSC was homogeneous with a well-established diagnosis. The general characteristics of our patients resemble those found in other countries with a male predominance, a median onset of the disease around 40 years of age, and a strong association with IBD.[3] However, among patients with IBD, the proportion of Crohn's disease (51%) was higher than usually reported.[29,30] This is probably related to the presence of a gastroenterology unit with a special interest in Crohn's disease in our institution. The topographic distribution of biliary involvement into intra- and extrahepatic (84%), intrahepatic only (16%), and extrahepatic only (0%) was also in keeping with other reports (>50%, <25%, and <5%, respectively).[3] Over a mean follow-up period of 4 years, our study including 64 patients has revealed two distinct radiologic disease courses: stability (42% of patients) and worsening (58% of patients). Worsening, as demonstrated by a marked increase in grade of intra- and extrahepatic bile duct strictures, degree of dilatation of the IHBD, and development of PH occurred rapidly (between 1 and 3 years in 95% of cases). We identified independent predictive radiologic features of disease progression, such as dilatation of the IHBD, dysmorphy, PH, and parenchymal enhancement heterogeneity, with which we created two radiologic scores (with and without gadolinium) that demonstrated similar performance. Nearly 90% of patients with radiologic worsening had an elevated score, whereas nearly 85% of patients with low scores had stable disease. Interestingly, risk of progression appears to depend mainly on

the effects of the biliary disease on the liver parenchyma (dysmorphy, PH, and parenchymal enhancement heterogeneity). A purely stenotic disease affecting the biliary tree, even if severe, seems to have a lower risk of progression. Indeed, severe stricture (>75%) of extrahepatic bile ducts was not associated with worsening. This finding appears to be counterintuitive, especially in the case of severe stricture of the CBD (37.5% at entry in the study). A dominant stenosis, as defined using ERC (diameter of less than 1.5 mm of the CBD and/or less than 1.0 mm of a hepatic duct within 2 cm of the bifurcation), has been reported to be a factor of poor clinical outcome.[19] Of note is the fact that we did not include the dominant stenosis parameter in our interpretation standard model because the ERC definition is not applicable, given the spatial resolution of 3D MRC (voxel size: $1 \times 1 \times 1$ mm).

An explanation why severe strictures on MRC lack prognostic value could be that MRC is unable to assess the strength of stricture, as opposed to ERC, which puts bile ducts in tension and thus reveals long-standing tight, fixed strictures. However, it should be kept in mind that, even with ERC, the prognostic value of dominant stenoses is a matter of debate, because a lack of correlation between biochemical cholestasis and presence of dominant stenoses has been reported.[31] Moreover, CBD strictures are rarely unique and other lesions may play a significant role.

PSC is a clinically polymorphic inflammatory disease affecting bile ducts that can lead to fibrosis and secondary biliary cirrhosis. This polymorphism translates into a variable combination of biliary and parenchymal damage on radiologic studies. Slight disease with little risk of progression seems to be characterized by biliary strictures, mainly of the IHBD, without dilatation or parenchymal injury, and could reflect a barely obstructive and fibrosing disease. By contrast, severe disease, with a greater risk of progression, seems to be characterized by dilatation of the IHBD and liver parenchymal injury and could be the result of biliary stasis with more marked chronic obstruction, leading to hepatic fibrosis. In addition, it may be hypothesized that abnormal peribiliary and parenchymal enhancement could be related to more active stages of the disease, especially in terms of inflammation and vascular remodeling.

The development of five tumoral lesions among these 64 patients (7.8%) is concordant with other reports (3.5%-10%[19,21]). The mechanisms of carcinogenesis in PSC are rather complex,[2,32] and the occurrence of a tumoral lesion may reflect more a complication than an evolution of the disease. Administration of gadolinium could remain of interest in the search for, and characterization of, complications.

End-stage cirrhosis caused by PSC is characterized by a dysmorphy with lobulation of the liver contours, atrophy of some segments (where the biliary disease predominates), and hypertrophy of more-spared segments.[33,34] Our patients with cirrhosis presented these features. The gallbladder was dilated in 39% of our patients on the first MRI, in accord with data presented by Said et al.,[35] showing a significant increased gallbladder volume in patients with PSC both fasting and after a meal. Reasons for this are still unknown, but mucosal dysfunction resulting from chronic cholecystitis may play a role.

Our study has some limitations. First, the MRI was performed for diagnostic purposes in 21 patients only (33%). The remaining patients underwent their first MRI as part of their follow-up (implementation of 3D MRC in 2002 in our center, first diagnostic imaging performed in another center, diagnosis based on ERC or on liver biopsy, and so on). Second, we did not perform an inter- and intraobserver concordance study. However, the 3D MRC techniques had been validated by the meta-analysis of Dave et al.[36] Last, it remains to be determined whether or not this radiologic progression translates into clinical events and, ultimately, into decreased transplant-free survival.

In conclusion, our study demonstrates a radiological progression in a majority of patients after a median follow-up of 4 years. Use of our interpretation standard model could help radiologists to analyze MRIs in patients with PSC. The calculation of one or two simple radiologic scores (depending on gadolinium administration) provides information on the risk of radiologic progression. An external validation of these scores is needed and the correlation with clinical outcome has to be determined.

Acknowledgment: The authors thank Louisa Azizi, Chantal Housset, and Maïté Lewin for their valuable advice and support.

References

1. Molodecky NA, Kareemi H, Parab R, Barkema HW, Quan H, Myers RP, Kaplan GG. Incidence of primary sclerosing cholangitis: a systematic review and meta-analysis. Hepatology 2011;53:1590-1599.
2. Krones E, Graziadei I, Trauner M, Fickert P. Evolving concepts in primary sclerosing cholangitis. Liver Int 2012;32:352-369.
3. Chapman RW, Fevery J, Kalloo A, Nagorney DM, Boberg KM, Shneider B, Gores GJ; American Association for the Study of Liver Diseases. Diagnosis and management of primary sclerosing cholangitis. Hepatology 2010;51:660-678.

4. European Association for the Study of the Liver. EASL Clinical Practice Guidelines: management of cholestatic liver diseases. J Hepatol 2009; 51:237-267.
5. Chapman RW, Arborgh BA, Rhodes JM, Summerfield JA, Dick R, Scheuer PJ, Sherlock S. Primary sclerosing cholangitis: a review of its clinical features, cholangiography, and hepatic histology. Gut 1980;21:870-877.
6. Majoie CB, Reeders JW, Sanders JB, Huibregtse K, Jansen PL. Primary sclerosing cholangitis: a modified classification of cholangiographic findings. AJR Am J Roentgenol 1991;157:495-497.
7. Craig DA, MacCarty RL, Wiesner RH, Grambsch PM, LaRusso NF. Primary sclerosing cholangitis: value of cholangiography in determining the prognosis. AJR Am J Roentgenol 1991;157:959-964.
8. Vitellas KM, El-Dieb A, Vaswani KK, Bennett WF, Tzalonikou M, Mabee C, et al. MR cholangiopancreatography in patients with primary sclerosing cholangitis: interobserver variability and comparison with endoscopic retrograde cholangiopancreatography. AJR Am J Roentgenol 2002;179:399-407.
9. Vitellas KM, Enns RA, Keogan MT, Freed KS, Spritzer CE, Baillie J, Nelson RC. Comparison of MR cholangiopancreatographic techniques with contrast-enhanced cholangiography in the evaluation of sclerosing cholangitis. AJR Am J Roentgenol 2002;178:327-334.
10. Angulo P, Pearce DH, Johnson CD, Henry JJ, LaRusso NF, Petersen BT, Lindor KD. Magnetic resonance cholangiography in patients with biliary disease: its role in primary sclerosing cholangitis. J Hepatol 2000;33:520-527.
11. Berstad AE, Aabakken L, Smith HJ, Aasen S, Boberg KM, Schrumpf E. Diagnostic accuracy of magnetic resonance and endoscopic retrograde cholangiography in primary sclerosing cholangitis. Clin Gastroenterol Hepatol 2006;4:514-520.
12. Fulcher AS, Turner MA, Franklin KJ, Shiffman ML, Sterling RK, Luketic VA, Sanyal AJ. Primary sclerosing cholangitis: evaluation with MR cholangiography—a case-control study. Radiology 2000;215:71-80.
13. Vitellas KM, Keogan MT, Freed KS, Enns RA, Spritzer CE, Baillie JM, Nelson RC. Radiologic manifestations of sclerosing cholangitis with emphasis on MR cholangiopancreatography. Radiographics 2000; 20:959-975.
14. Ernst O, Asselah T, Sergent G, Calvo M, Talbodec N, Paris JC, L'Herminé C. MR cholangiography in primary sclerosing cholangitis. AJR Am J Roentgenol 1998;171:1027-1030.
15. Sodickson A, Mortele KJ, Barish MA, Zou KH, Thibodeau S, Tempany CM. Three-dimensional fast-recovery fast spin-echo MRCP: comparison with two-dimensional single-shot fast spin-echo techniques. Radiology 2006;238:549-559.
16. Kim WR, Therneau TM, Wiesner RH, Poterucha JJ, Benson JT, Malinchoc M, et al. A revised natural history model for primary sclerosing cholangitis. Mayo Clin Proc 2000;75:688-694.
17. Kim WR, Poterucha JJ, Wiesner RH, LaRusso NF, Lindor KD, Petz J, et al. The relative role of the Child-Pugh classification and the Mayo natural history model in the assessment of survival in patients with primary sclerosing cholangitis. Hepatology 1999;29:1643-1648.
18. Olsson RG, Asztély MS. Prognostic value of cholangiography in primary sclerosing cholangitis. Eur J Gastroenterol Hepatol 1995;7:251-254.
19. Rudolph G, Gotthardt D, Klöters-Plachky P, Kulaksiz H, Rost D, Stiehl A. Influence of dominant bile duct stenoses and biliary infections on outcome in primary sclerosing cholangitis. J Hepatol 2009;51:149-155.
20. Stiehl A, Rudolph G, Klöters-Plachky P, Sauer P, Walker S. Development of dominant bile duct stenoses in patients with primary sclerosing cholangitis treated with ursodeoxycholic acid: outcome after endoscopic treatment. J Hepatol 2002;36:151-156.
21. Ponsioen CY, Vrouenraets SM, Prawirodirdjo W, Rajaram R, Rauws EA, Mulder CJ, et al. Natural history of primary sclerosing cholangitis and prognostic value of cholangiography in a Dutch population. Gut 2002;51:562-566.
22. Petrovic BD, Nikolaidis P, Hammond NA, Martin JA, Petrovic PV, Desai PM, Miller FH. Correlation between findings on MRCP and gadolinium-enhanced MR of the liver and a survival model for primary sclerosing cholangitis. Dig Dis Sci 2007;52:3499-3506.
23. Hoeffel C, Azizi L, Lewin M, Laurent V, Aubé C, Arrivé L, Tubiana JM. Normal and pathologic features of the postoperative biliary tract at 3D MR cholangiopancreatography and MR imaging. Radiographics 2006;26:1603-1620.
24. Awaya H, Mitchell DG, Kamishima T, Holland G, Ito K, Matsumoto T. Cirrhosis: modified caudate-right lobe ratio. Radiology 2002;224: 769-774.
25. MacCarty RL, LaRusso NF, May GR, Bender CE, Wiesner RH, King JE, Coffey RJ. Cholangiocarcinoma complicating primary sclerosing cholangitis: cholangiographic appearances. Radiology 1985;156:43-46.
26. Carey V, Zeger SL, Diggle PJ. Modelling multivariate binary data with alternating logistic regressions. Biometrika 1993;80:517-526.
27. Moons KG, Harrell FE, Steyerberg EW. Should scoring rules be based on odds ratios or regression coefficients? J Clin Epidemiol 2002;55: 1054-1055.
28. Steyerberg EW, Harrell FE, Jr., Borsboom GJ, Eijkemans MJ, Vergouwe Y, Habbema JD. Internal validation of predictive models: efficiency of some procedures for logistic regression analysis. J Clin Epidemiol 2001;54:774-781.
29. Kingham JG, Kochar N, Gravenor MB. Incidence, clinical patterns, and outcomes of primary sclerosing cholangitis in South Wales, United Kingdom. Gastroenterology 2004;126:1929-1930.
30. Escorsell A, Parés A, Rodés J, Solis-Herruzo JA, Miras M, de la Morena E. Epidemiology of primary sclerosing cholangitis in Spain. Spanish Association for the Study of the Liver. J Hepatol 1994;21:787-791.
31. Björnsson E, Lindqvist-Ottosson J, Asztely M, Olsson R. Dominant strictures in patients with primary sclerosing cholangitis. Am J Gastroenterol 2004;99:502-508.
32. Blechacz B, Gores GJ. Cholangiocarcinoma: advances in pathogenesis, diagnosis, and treatment. Hepatology 2008;48:308-321.
33. Dodd GD, 3rd, Baron RL, Oliver JH, 3rd, Federle MP. End-stage primary sclerosing cholangitis: CT findings of hepatic morphology in 36 patients. Radiology 1999;211:357-362.
34. Bader TR, Beavers KL, Semelka RC. MR imaging features of primary sclerosing cholangitis: patterns of cirrhosis in relationship to clinical severity of disease. Radiology 2003;226:675-685.
35. Said K, Edsborg N, Albiin N, Bergquist A. Gallbladder emptying in patients with primary sclerosing cholangitis. World J Gastroenterol 2009;15:3498-3503.
36. Dave M, Elmunzer BJ, Dwamena BA, Higgins PD. Primary sclerosing cholangitis: meta-analysis of diagnostic performance of MR cholangiopancreatography. Radiology 2010;256:387-396.